

*XVII IMEKO World Congress
Metrology in the 3rd Millennium
June 22–27, 2003, Dubrovnik, Croatia*

DETECTION AND CLASSIFICATION OF AIR BUBBLE SILHOUETTES IN PIV-IMAGES

Marjo Lahti, Kalle Marjanen, Heimo Ihalainen

Measurement and Information Technology, Tampere University of Technology, Finland, Signal Processing Laboratory, Tampere University of Technology, Finland

Abstract – A practical method for detection, segmentation and classification of the air bubble silhouettes in Particle Image Velocimeter (PIV) images is proposed. Air bubbles that are in focus plane have sharper edges and lower intensities than defocused bubbles. Detection and segmentation is based on estimating the local variances and comparing these with the local intensities. After detection and segmentation different statistics describing the size and shape of the bubbles can be measured. An example of using this method is provided.

Keywords: classification, air bubble, PIV.

1. INTRODUCTION

A PIV-system [1] measures velocity by determining seed particle displacements over short time intervals. Particles are illuminated with a laser to create a light plane and images are taken by digital camera. Consecutive images are used to calculate an estimate of the flow field by cross-correlations [2][3]. Sometimes it is of interest to find also other objects than those small seed particles used for flow field calculation. Detection of air bubbles is such a task [4].

The shape of the air bubbles can be estimated from conventional PIV images. Large changes in intensities and saturation of the detector due to light scattering and reflections can make this a challenging task. One solution for this problem is use back lighting. In back light image the background light penetrates throughout water and reflects off from air bubbles. In the acquired image the bubbles are shown as shadows. Bubbles that are in focus plane have lower intensities and sharper borders than defocused bubbles. Information of intensity and local variances is used in detection and segmentation.

The features of the air bubble silhouettes are computed from the segmented image. These features contain the coordinates of the centre of mass, the area, the orientation and the major and minor axis lengths of the bubbles. These features are computed from an image series under the same circumstances. For example the size distribution or the joint distribution between size and centre of mass positions is estimated. These distributions are used in further analysis of the flow properties.

The PIV-system in the Laboratory of Energy and Process Engineering in Tampere University of Technology was used in the experiments.

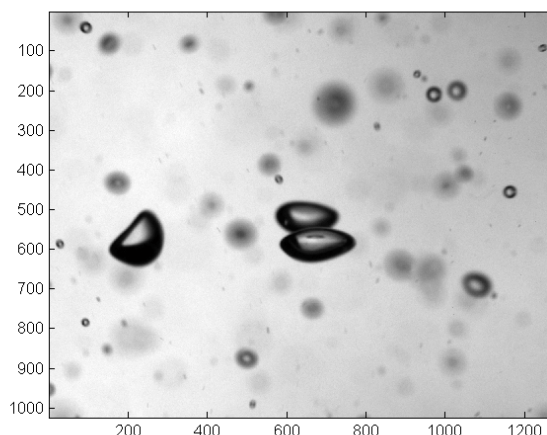


Fig. 1. Flow containing air bubbles. Silhouettes in the flow are shown as darker areas in the image.

The experimental set-up included a cylindrical mixing vessel, which was placed in a rectangular container filled with water to prevent reflections on the walls of the vessel. A four-blade turbine was in the centre of the vessel close to bottom, and the bubble injector is placed in the middle of the bottom. The gas bubbles upward, and gas flow is controlled by a mass flow rate control valve [6].

To get the time series information, i.e. how the bubble sizes vary with the time and different circumstances, the image series containing 50 or more images are taken. The shooting frequency has been 8 Hz and the parameter that was changed was; the rotation speed of the blender, the gas flow rate from the injector or camera.

The bubble size distribution, the minor and major axis length distributions, mass centre coordinates and orientation are determined from each image series based on detection and segmentation of air bubble silhouettes.

This time series information together with the fluid velocity measured other ways produces additional information of the bubble flow.

2. DETECTION AND SEGMENTATION OF AIR BUBBLE SILHOUETTES

Before any kind of relative measurement can be done the air bubble silhouettes have to be detected and segmented with some reliable method. The detection of the air bubbles

is based on two main assumptions. The first assumption is that the air bubbles have darker areas than the background, which in this case is the water. The darker areas of the air bubbles are caused by the light reflection and scattering. This effect depends from the mediums and the angle between the light and the boundary of the bubble. The second assumption is that the air bubbles that are in the focus plane tend to have sharp borders. This is due to the fact that when an optical system is in the focus the *MTF* (Modulation Transfer Function) of the lens system is maximised and therefore a maximum amount of the scene variance is passed to the rest of the system.

These assumptions are the source of a two-dimensional feature space that contains the local mean and the local variance. This feature space is assumed to contain several classes that are the background, the objects in the focus and the objects out of the focus. The clusters in the space can be found by k-means algorithm or some similar method.

2.1 Pre-processing of the air bubble image

Consider an image taken from a source that has equal intensity in the camera *FOV* (Field of Vision). The obtained image should have equal grey values if the system noise is not considered. In the real systems there is always some sort of change in the local mean of the image intensity. These variations are mainly caused by the uneven illumination of the source and the properties of the optics. The combined effect of the illumination and the optics, usually a low frequency phenomenon, has to be removed before the local mean can be used in any global operations. This effect is estimated with a polynomial fit that uses only the brighter parts of the image, that is the water not the air bubble silhouettes. This polynomial is evaluated over the whole image and is subtracted from the original image.

2.2 Local mean and variance estimation

The estimates of the local mean and the local variance are computed with a moving estimate. A small window, say 5 x 5, is moved over the image and the parameters are computed from its current area. The common formulas for the sample mean and the sample variance can be used, but for computational efficiency a slight variation was chosen.

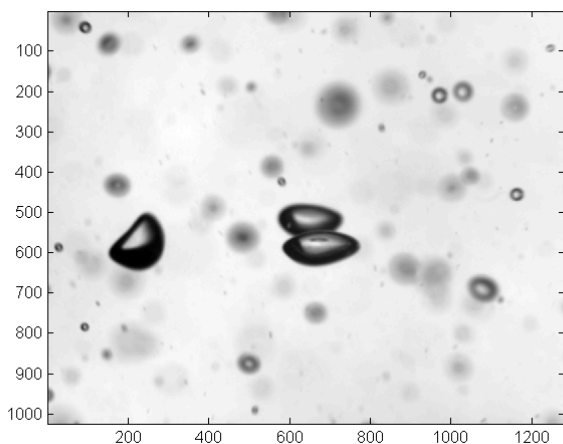


Fig. 2. Result of the local mean estimation after the polynomial background trend is removed.

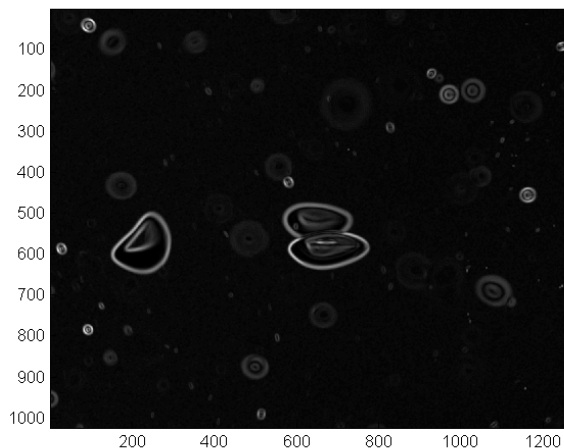


Fig. 3. Result of the local variance estimation: sharp borders that have higher variance are shown in brighter intensity.

The filter used in moving mean computation is usually an *m x n* box-filter *h* having equal weights that adds to one.

The estimation of the local variance is based on the well-known equation of the variance.

$$\sigma_X^2 = E[(X - \mu_X)^2] = \Psi_X^2 - \mu_X^2, \tag{1}$$

where the operator *E* denotes the expectation value, *X* is the value of the variable, μ_X expectation value of *X* and Ψ_X^2 is the quadratic mean of the variable *X*.

From the (1) it can be seen that the estimation of the local variance can be computed with the difference of the local quadratic mean and the local squared mean.

2.3 Segmentation using the variance and the intensity

The segmentation is based on the two assumptions considering the high variance and low intensity of air bubbles in focus. A two-dimensional histogram of the local mean and variance estimates is computed. This two-dimensional feature space does not contain any clear distinct classes like the background, object in focus and object out of focus. The clearest ‘class’ is the background that is the water. The background *pdf* can be estimated with a two-dimensional *pdf* and the areas not belonging to the estimated background *pdf* are considered to be the objects of interest. The discrimination between the objects on focus and out of focus is a matter of choice. There is no clear separation between these two classes.

3. CLASSIFICATION OF AIR BUBBLE SILHOUETTES

A set of measurements is computed for each detected bubble. Cross-sectional area is the number of pixels in bubble. Centroid is x- and y-coordinates of the centre of mass of cross-section of the bubble. The length in pixels of the major axis and the minor axis of the ellipse that has the same second-moments as the bubble and the angle in degrees between the x-axis and the major axis of the ellipse that have the same second-moments as bubble region.

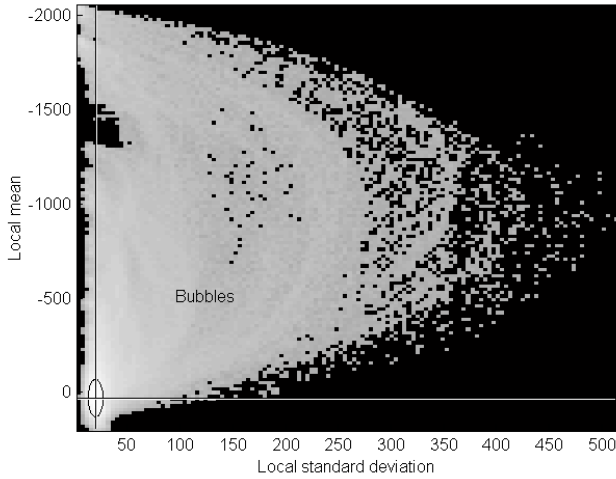


Fig. 4. Classification of the PIV image to the bubbles and the background using two-dimensional features space. The features are local mean and the local variance. The background is shown in the lower left corner. The lines are positioned at the estimated mean of the background. 99,7 % of the background should be inside the ellipse.

4. EXAMPLE

To get the time series information an image series containing 50 images is used as an example. Detection and segmentation of the bubbles are done using procedures described in section 2 and the classification is done based on section 3.

All dark areas, whose local variances are high enough, are detected as bubbles in the image. Some objects like a seed particle in the flow is also detected as a bubble. Therefore, all small objects, which have area smaller than 50 pixels are ignored from further calculations.

The size of the bubbles, centre of mass, the major and minor axes and orientation is computed for every bubble in each image. These measures are a function of time and place.

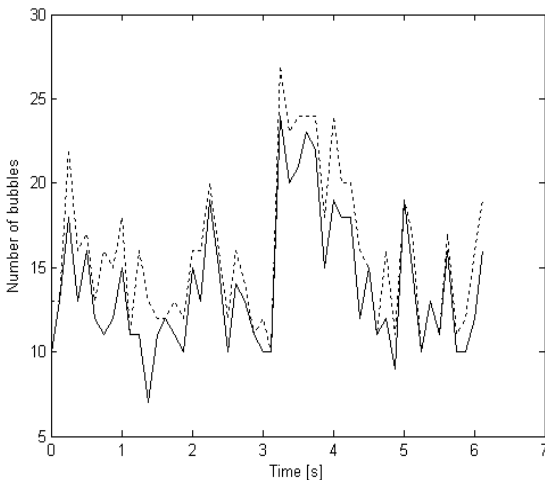


Fig. 5. The number of the bubbles in the images. The dotted line (upper) shows the number of all detected objects in the images. The solid line shows the number of objects when small particles are removed from the results.

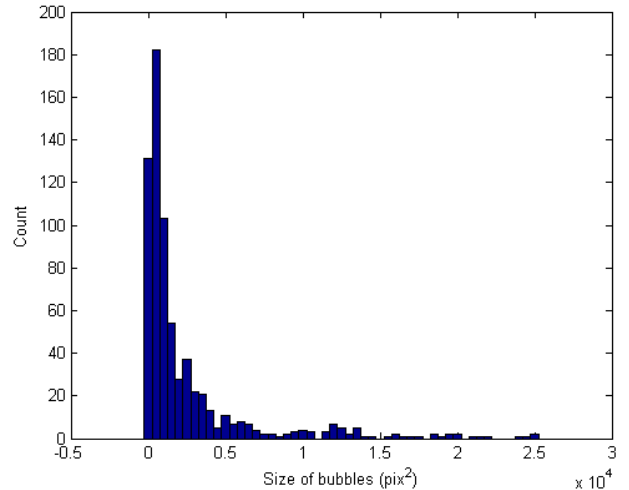


Fig. 6. The bubble size distribution calculated from the image series

Some of the classification results are visualized. These include the number of bubbles in each image, the size distribution of the bubbles from the whole time series, the local major axis length and orientation of the bubbles and the ratio of major axis length to minor axis length as a function of orientation.

Fig 5. presents the effect of the removal of the small objects. The number of detected bubbles is not changed much. This is due the fact that there are no seed particles in this test series.

Fig 6. shows the histogram of the bubbles in all images. Statistics such as the mean or standard deviation can be computed from bubble size histogram. Statistics can be compared between different time series and single images.

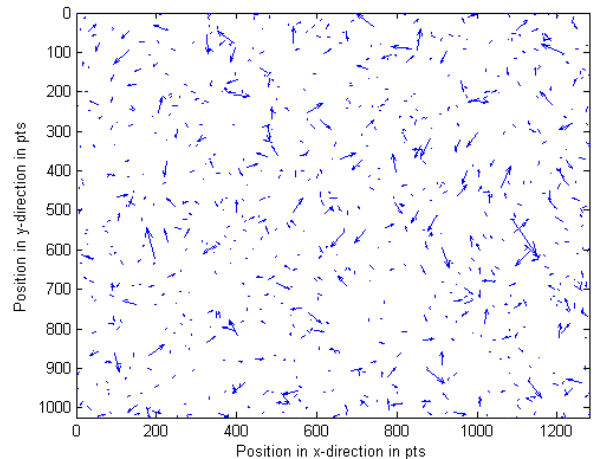


Fig. 7. The mass centre coordinates of the bubbles together with major axis -length and orientation information.

In Fig 7. the mass centre coordinates of the bubbles together with major axis -length and orientation information are shown. Arrow length presents the length of the major axis and the direction of the arrow presents the orientation. Arrows are placed on the estimated mass centre of the bubbles. It seems that the number of the images is insufficient to make statistical conclusion with non-parametric methods. From this can be calculated the local estimates of orientation.

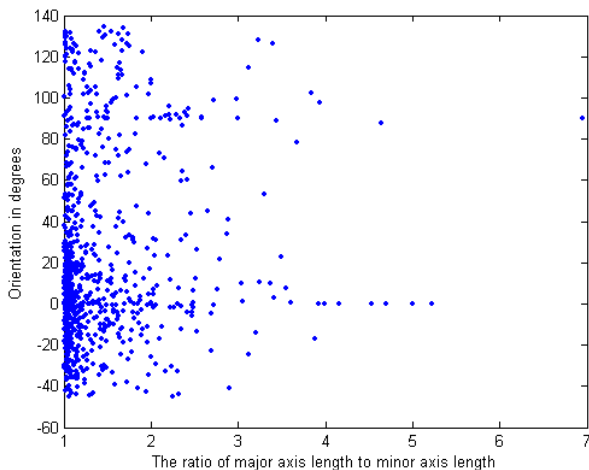


Fig. 8. Orientation as a function of the ratio of major axis length to minor axis length.

Fig 8. shows that in our case more elliptical bubbles are directed in horizontal or vertical direction. It is assumed that this phenomenon is caused by the experimental set-up.

5. CONCLUSIONS

The back lighted images seem to be more suitable for the air bubble detection, segmentation and classification with image processing methods than conventional PIV-images. This is due to the fact that the variation in bubble intensity is smaller than when using lasers. Method described above can be automated to handle large datasets obtained from the PIV-system.

It should be noticed that the results are comparable when same kind of cameras, optics and imaging geometry is used.

It is possible to get a lot of information, which can be later analysed with different statistical methods. This information can be combined with the estimated flow field.

Further work is to combine the time series information from detecting and classifying the air bubble silhouettes to the flow field information measured in other ways.

REFERENCES

- [1] M. Raffel, C Willert, J. Kompenhans, "Particle image velocimetry: a practical guide", *Springer-Verlag*, 1998.
- [2] S. P. McKenna, W. R. McGillis, "Performance of digital image velocimetry processing techniques," *Experiments in Fluids* 32 (2002) pp. 106-115, Springer-Verlag 2002
- [3] H. T. Huang, H. E. Fiedler, J. J. Wang, "Limitation and improvement of PIV, Part II: Particle image distortion, a novel technique," *Experiments in Fluids* 15 (1993) pp. 263-273, Springer-Verlag 1993.
- [4] I. Dias, M.L. Riethmuller, "PIV in Two-Phase Flows: Simultaneous Bubble Sizing and Liquid Velocity Measurements", *Proc. Turbulent Shear Flow Phenomena*, St. Barbara, California, USA, 1999.
- [5] K. R. Castleman, "Digital image processing", *Prentice-Hall* 1996.
- [6] M. Honkanen, "Turbulent multiphase flow measurements with particle image velocimetry: Application to bubble flow", MSc. Thesis, Tampere University of Technology, Energy and Process Engineering, Tampere, Finland, 2002

Authors: Marjo Lahti, Measurement and Information Technology, Tampere University of Technology, P.O. Box 692, FIN-33101 Tampere, FINLAND, marjo.lahti@tut.fi. Kalle Marjanen, Signal Processing Laboratory, Tampere University of Technology, P.O. Box 553, FIN-33101 Tampere, FINLAND, kalle.marjanen@tut.fi. Heimo Ihalainen, Measurement and Information Technology, Tampere University of Technology, P.O. Box 692, FIN-33101 Tampere, FINLAND, heimo.ihalainen@tut.fi